# PRE-STRESSED REINFORCED CONCRETE ELEMENTS UNDER BLAST LOADING: NUMERICAL ANALYSIS AND SHOCK TUBE TESTING

CHRISTOPH ROLLER, MALTE VON RAMIN & ALEXANDER STOLZ
Fraunhofer Institute for High-Speed Dynamics, Ernst-Mach Institut (EMI), Germany

ABSTRACT
Advanced numerical and experimental analysis of complex structural loading conditions is presented within this paper. Major building components reinforced concrete (RC) walls are investigated with regard to their detonation resistance in various pre-stressed states. A multi-step simulation approach using successively both implicit and explicit integration schemes is followed to model the coupled static and dynamic loading. The simulation results underline the validity of the chosen modelling approach. A comparison of experimental and numerical values shows good agreement for deformation behaviour as well as for damage pattern. Beyond these predictive calculations further parameter variations indicate the dependency of highly dynamic structural response on quasi-static pre-load conditions.
*Keywords: blast loading, hydrocode simulation, shock tube, pre-stressed reinforced concrete.*

## 1 INTRODUCTION

Nowadays, an increased number of natural and manmade hazards (fire, impact, explosion [1]) needs to be considered during design phase of new buildings and requires reassessment of existing structures. Focusing on events at time range of shock phenomena, the main load bearing components have to withstand the extraordinary load conditions up to a level where fatal debris ejection is prevented and integrity as well as stability of the constructions is ensured. To cover realistic built-in stress states, analysis may not only focus on the exceptional load case itself, but include common design loads. This is the part structural engineers are quite familiar with. They deal with quasi-static loads such as live and dead loads on a day-to-day basis, even in combination with dynamic loading such as earthquake motion [2], [3]. Common approaches from structural dynamics such as response spectra [4], [5] are well established in this field and embedded in building standards [6]. In contrast, design against high-speed phenomena such as impact and explosion is rarely standardized. These phenomena rather belong to the field of natural scientists and thus analysis methods differ from common engineering practice. Besides sophisticated experimental trials, advanced numerical simulation offer the best alternative to investigate resistance of structural components under this combined static–dynamic loading in detail [7]. However, finite element calculations of structural components usually focus on single or at least similar load regimes. While common structural engineering problems can numerically be solved with implicit integration schemes, the shock problems are solved using explicit time integration. A recent study on exposed reinforced concrete (RC) walls includes a combination of both to tackle the given transient problem. The numerical analysis and related trials are described briefly in the following.

## 2 SIMULATION APPROACH AND VALIDATION

The investigations conducted within the ANSYS Workbench environment comprise four different initial load conditions with three dynamic load regimes each. Besides purely vertical, purely horizontal and combined vertical plus horizontal pre-load, configurations without any pre-load are investigated. The latter serve as reference to classify the influence

WIT Transactions on The Built Environment, Vol 209, © 2022 WIT Press
www.witpress.com, ISSN 1743-3509 (on-line)
doi:10.2495/HPSU220151

of the single pre-load configurations on the structural response of the exposed RC-walls. Table 1 gives an overview about the scope of the investigations.

Table 1: Scope of investigations.

| Configuration | Pre-load | | Dynamic load |
|---|---|---|---|
| | Vertical – n0 | Horizontal – p0 | DIN 13123-1 [8] |
| n0 | √ | x | EPR1 |
| | √ | x | EPR2 |
| | √ | x | EPR3 |
| n0p0 | √ | √ | EPR1 |
| | √ | √ | EPR2 |
| | √ | √ | EPR3 |
| p0 | x | √ | EPR1 |
| | x | √ | EPR2 |
| | x | √ | EPR3 |
| 0 | x | x | EPR1 |
| | x | x | EPR2 |
| | x | x | EPR3 |

The modelled RC-walls measure 186 cm in height, 60 cm in width and 12.5 cm over thickness. Concrete body as well as reinforcement, consisting of steel bars and shear links, are individually discretized according to their dimensions in full-scale (see Fig. 1). Supports at top and bottom of the bodies are modelled using translational and rotational boundary conditions. Pre-load conditions are applied to the corresponding surfaces via appropriate stress boundary conditions, too. Gauge points are defined at significant locations at mid-span and on top of the concrete body for analysis of displacement and stress histories.

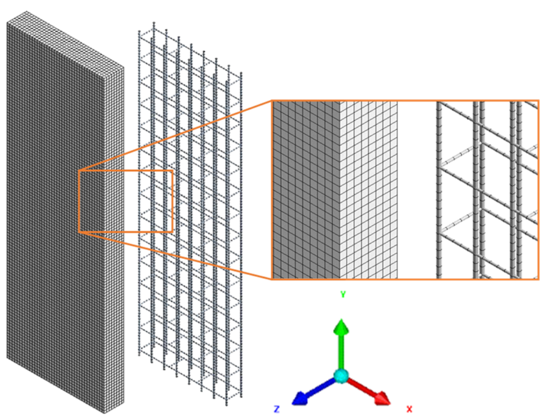

Figure 1: Numerical model of RC-wall with discrete reinforcement.

## 2.1 Combined loading–combined solvers

Analysis of such walls under combined quasi-static and highly dynamic loading requires more than one time integration scheme to produce efficient simulations. Thus, a coupled multi-step simulation approach using both implicit and explicit solvers is followed for the present transient problem.

Based on the developed model, first the quasi-static load case is computed as a pre-stressed analysis using the ANSYS Mechanical APDL solver. Simulation results such as vertical and horizontal deformation plus vertical stress are identified for matching of data with next steps. Second, the data including geometry model, mesh size and analysis settings is transferred to the explicit dynamics module. The information from pre-stress analysis is applied via displacement-orientated initial condition to position the explicit nodes in a pre-defined time. During the initialization strains and stresses are computed by the ANSYS Explicit STR solver as usual.

To change the calculation from a dynamic solution to a relaxation iteration which converges to a state of stress equilibrium a static damping constant $R$ is specified. Depending on the average time step $ts$ and the longest period of the system's motion $T$ constant $R$ can be chosen from eqn (1) for ratios of $ts \ll T$:

$$R = 2 \cdot \left(\frac{ts}{T}\right) \tag{1}$$

Thus, an intermediate step for determination of $T$ is integrated into the process. The Modal module is linked to the static structural system transferring all set-up and solution data from pre-stress analysis. Running the modal analysis gives the required first natural period. Taking into account an average value for $ts$ from a preliminary explicit calculation without static damping $R$ amounts to a value of $2.6710^{-4}$ ms in this case which is within the recommended range.

The third step includes the transfer of the computed data to the hydrocode ANSYS AUTODYN [9]. Here, a change of material models is required. Although the explicit dynamics solver from the previous step uses the same explicit solver as hydrocode, the material data is linked to the static structural module and thus the solver refers to "implicit models". These models are not designed for transient problems in the range of shock loading. Thus, well established material models that cover phenomena as compaction and strain rate effects are applied for concrete and steel, namely RHT [10] and Johnson–Cook [11].

To discuss the intended equilibrium state after pre-load initiation, Fig. 2 exemplarily shows the displacement-time history for the top face centre of the RC-wall under combined pre-load determined by the single simulation steps. Comparing results from implicit and explicit pre-simulation, it is apparent that the explicit curve is neither balanced nor does it match with the static solution. Taking into account the hydrocode calculation with implicit material models, it is clear that this mismatch cannot be related to the different solvers, since this curve does agree well with the implicit solution. It is assumed that this difference results from an insufficient bonding between steel beam elements and concrete volume body in the explicit dynamics module. Merging the nodes is realized during implicit simulation set-up and via the corresponding option for all unstructured nodes within the hydrocode environment, but both is not an option for the explicit dynamics module. Since the focus is on a coupled simulation using the hydrocode, this short coming is neglected.

However, comparing solutions from the hydrocode the expected influence resulting from different material models is observed. To achieve the intended initial displacement the applied pre-load is linearly reduced in the hydrocode. The resulting curve approves this approach in matching the targeted implicit curve.

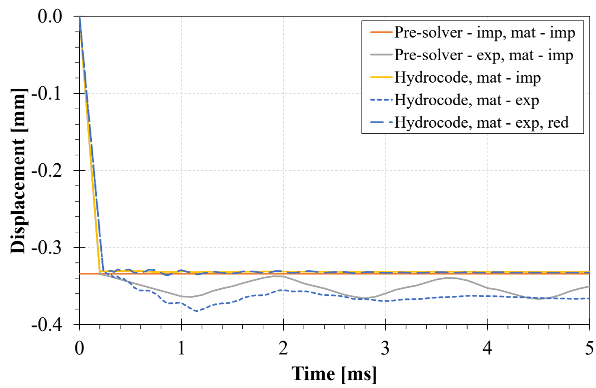


Figure 2: Evolution of vertical displacement at top of RC-wall in order to achieve equilibrium state.

## 2.2 Validation of approach

Results of shock tube tests are used to validate the simulation approach with regard to chosen discretization, boundary conditions and material models. The trials are conducted using the shock tube BlastStar [12] at Fraunhofer EMI facilities. Before being loaded with air pressure shock wave the RC-specimen have been pre-stressed perpendicular to as well as along the plate axis. To apply quasi-static bending load perpendicular to the plate axis, the shock tube has been enhanced by installation of a ventilation adapter enabling over-pressure respectively low-pressure regimes. Comprehensive computation of structural and gas dynamics for ventilator and its mounting have been conducted with regard to the dynamic shock wave loading. To apply quasi-static compression load along the plate axis as well as to realize sufficient support conditions further design work has been necessary. Fig. 3 illustrates the developed supporting frame including dowel pins and pre-stressed rods in ways of technical drawing and final built-in state. Using these extra features, it is possible to apply pre-loads up to $p = 30$ kN/m$^2$ in horizontal and $N = 2{,}400$ kN in vertical direction.

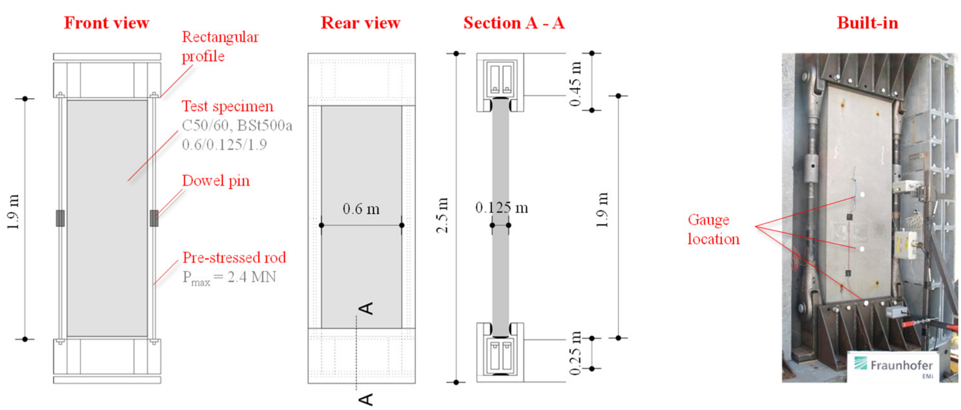


Figure 3: Test set-up for RC-walls under combined loading as construction detail (left) and in built-in state (right).

Main focus of the investigations is on deformation behaviour of the RC-wall, since the flexural strength is the decisive parameter for walls loaded by air shock pressure related to a far range detonation. Accordingly, an extensive instrumentation has been provided. Apart from pressure sensors for measurement of applied dynamic loading on the exposed face, laser and high-speed video equipment plus strain gauges have been installed on the opposite side for specification of the structural response.

First, maximum deformation of the single test series is observed. Fig. 4 contains the pair of values from numerical and experimental data source. The red diagonal represents the line where results of simulation and experiment are in conformity. The blue marks displayed in the diagram are located very close to that line for all types of pre-loading. This indicates that the particular results are in good correlation. Hence, the simulations are suitable for further analysis of the deformation behaviour.

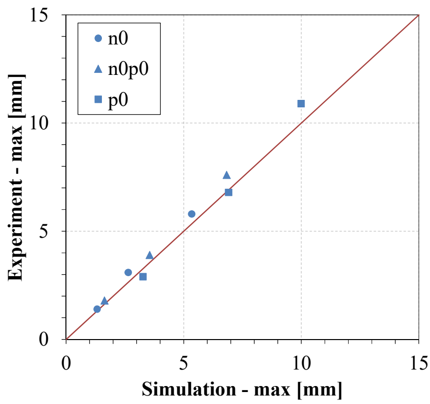


Figure 4: Comparison of numerically and experimentally determined maximum deflections.

A second significant parameter being used for validation is the emerging degree of damage. Most analysed configurations stayed in the damage-free elastic range. Only the configuration without any pre-load showed some crack initiation on the non-loaded side at increased dynamic loading due to tensile loading. Fig. 5 exemplarily compares damage pattern of the RC-elements after EPR3 loading [8]. The colour coding of the simulation results represents a strength related damage. Blue equals to intact concrete regions, whereas red represents regions with no residual strength left, meaning completely damaged regions. During previous studies it has been seen that green–yellow colour-coding is related with regions of crack formation. In the light of the above a good correlation between simulation and experiment is given here, too: Various horizontal cracks can be detected in mid-span. Based on these and the above mentioned conformity in results, it follows that the simulations provide sufficient predictive quality posse the ability of prognosis and can be used for further analysis.

## 3 INFLUENCE OF SINGLE LOAD LEVELS

To begin with, the computed first deflection for each static-dynamic loading is comparatively displayed in Fig. 6 for blast load EPR2 [8]. The reducing effect for the single pre-load conditions is clearly given. It is shown in particular that the deflection curve resulting from

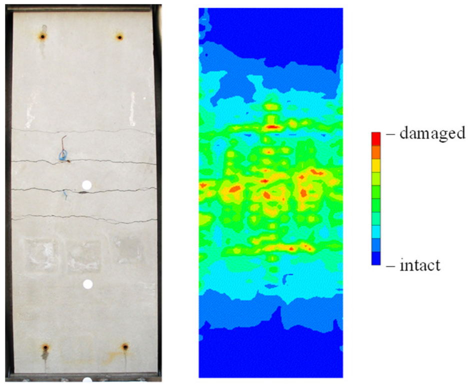


Figure 5: Degree of damage of the RC-plates after EPR3 [8].

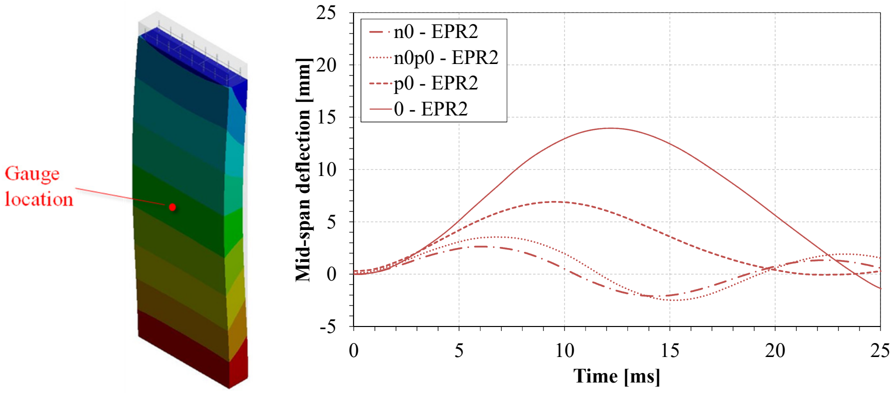


Figure 6: Comparison of numerically determined displacement-time histories for EPR2 [8] and gauge location.

combined pre-load cannot be extrapolated by superposition of the curves resulting from single pre-loads but that it lies in between them. More precisely, the behaviour due to combined pre-load is closer to the one from purely vertical pre-load. This phenomenon similarly appears for the configurations with decreased and increased blast loads. However, it has not been theoretically fully understood and needs to be studied further.

Focusing on the effect of the single pre-loads individually a number of parameter variations have been computed with different levels of pre-load and blast load. This also demonstrates the added value by using simulations, since any experimental parameter studies would consume a multiple amount of time and money.

### 3.1 Level of vertical pre-load

Starting from the vertical static compressive stress referred to above, the stress has been divided by two in a first variation and doubled in a second variation for each of the three dynamic explosion pressure classes. The result of the numerical investigation is given in terms of displacement-time histories (see Fig. 7 (left)). The previously noted effect can be confirmed by the parameter study: Increased vertical pre-load leads to decreased maximum deflection and vice versa. Additionally it is noted that the varying boundary conditions influence the natural oscillation behaviour: Increased vertical pre-load leads to decreased natural period (increased natural frequency) and vice versa.

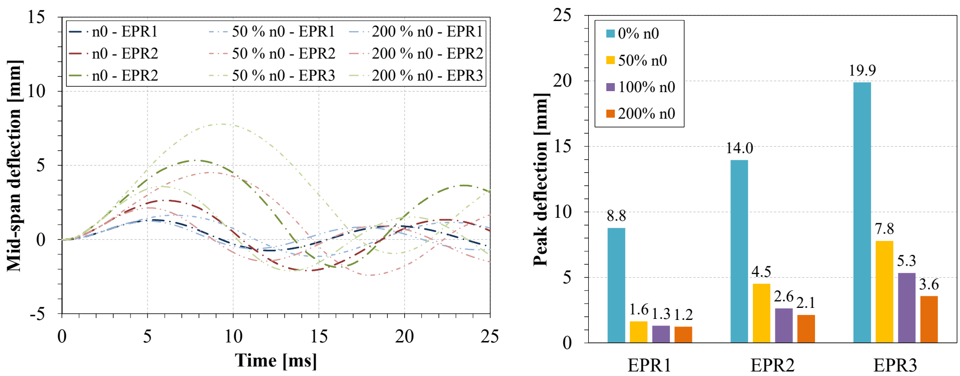


Figure 7: Comparison of numerically determined displacement-time histories for varying vertical pre-loads (left) and blast levels and of absolute maximum deflections with and without vertical pre-load variations for single dynamic blast levels (right).

To specify the effect further, the determined maximum deflections are compared with the ones from reference simulations without any pre-load. The comparison of absolute values in Fig. 7 (right) illustrates the significant influence of the vertical pre-load. At a dynamic load of 100 kPa (EPR2) for example the amplitude can be reduced from 14.0 mm down to 2.1 mm at highest vertical pre-load. This equals to a reduction down to 15% related to the reference configuration. In addition it is found that the degree of reduction also depends on the level of blast load: The mitigating effect decreases at increasing blast level. Generally a reduction between 13% and 39% is numerically detected.

It should be noted that the promising simulation results of decreased deformation have to be evaluated with care: Due to the dynamically induced bending deformation the initially axial pre-load becomes an eccentrically vertical load at increased bending stress. Thus, the risk of flexural buckling needs to be considered in building practice relevant design for combined static vertical and dynamic horizontal load. There is still research needs in this field.

## 3.2 Level of horizontal pre-load

In analogy to the previous variant analysis, for the horizontal pre-load the planar static compressive stress is divided by two on the one hand and doubled on the other hand, too. The result of the simulation runs is illustrated in way of displacement-time histories again, see Fig. 8 (left). In contrast to the situation of vertical pre-load it is not possible to confirm a steady effect. A decreased horizontal pre-load does lead to an increased maximum deflection, but so does an increased horizontal pre-load. It seems that a limited effect is acting here which is valid for a certain range of parameters only.

A significant influence on the natural period cannot be detected here and thus is assumed to be negligible for this parameter variation.

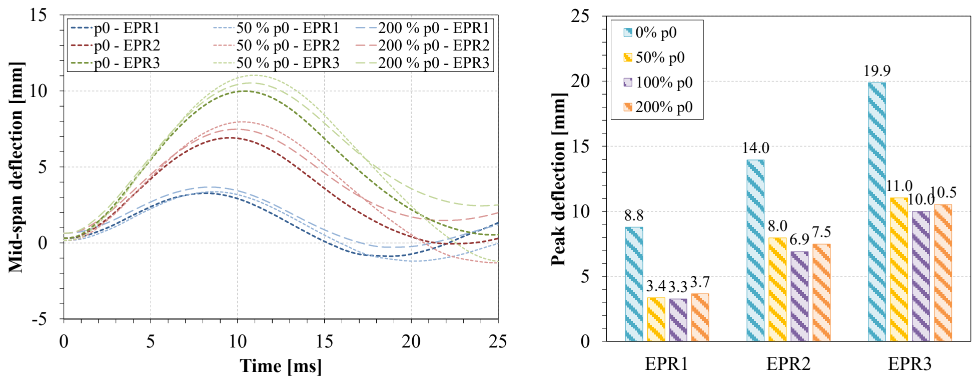


Figure 8: Comparison of numerically determined displacement-time histories for varying horizontal pre-loads and blast levels and of absolute maximum deflections with and without horizontal pre-load variations for single dynamic blast levels (right).

The absolute values of the computed maximum deflections are compared to the values from the reference simulation without any pre-load in Fig. 8 (right). On the one hand the diagram clearly illustrates the existing influence of the horizontal pre-load. On the other hand, the increased deflection is evidenced for both half and double horizontal pre-load. This is an effect that needs to be investigated further. A comparison with Fig. 8 indicates that the applied vertical pre-load affects the maximum deflection to a greater extend. Whereas a reduction between 13% and 39% is detected for the previous pre-load study, here values between 37% and 57% are noted. Additionally, it is found that the degree of reduction does not depend on the level of blast load for the horizontal pre-load: The mitigating effect becomes rather constant at increasing blast level.

## 4 CONCLUSIONS

Based on the parametric studies new findings are introduced in the field of pre-loaded protective structures. The combined experimental and numerical investigations outline the importance of considering initial stress states when dealing with blast-resistant design: Both vertical and horizontal pre-load significantly influence the structural response of exposed RC-walls. This includes but goes beyond characteristics such as peak deformation, oscillation and residual load capacity.

The coupled simulation approach provides realistic results for the investigated reinforced concrete members under complex loading conditions for both, deformation behaviour and damage pattern. Thus, the approach can be used for further investigations on this topic.

## REFERENCES

[1] Ibrahimbegovic, A., *Extreme Man-Made and Natural Hazards in Dynamics of Structures*, Springer: Dordrecht, Netherlands, 2007.

[2] Bachmann, H., *Erdbebensicherung von Bauwerken*, 2, überarbeitete Auflage. Birkhäuser Verlag: Basel, Switzerland, 2002.

[3] Butenweg, C. & Roeser, W., *Erdbebenbemessung von Stahlbetontragwerken nach DIN EN 1998-1*, Goris & Hegger, eds, Stahlbetonbau aktuell 2012 - Praxishandbuch, Bauwerk Verlag: Beuth, Berlin, Germany, 2012.

[4] Newmark, N.M. & Hall, W.J., *Earthquake Spectra and Design*, Berkeley, CA, USA, 1982.

[5] Chopra, A.K., *Dynamics of Structures*, 2nd ed., Prentice Hall: Upper Saddle River, NJ, USA, 2001.

[6] Deutsches Institut für Normung, DIN 4149:2005-04: Buildings in German earthquake areas – Design loads, analysis and structural design of buildings, Beuth, Berlin, 2005.

[7] Riedel, W. & Mayrhofer, C., Customized calculation methods for explosion effects on structural building components. *Int. Symp. on Structures under Earthquake, Impact and Blast Loading – IB'08*, Osaka University, Arata Hall, Osaka, Japan, 2008.

[8] Deutsches Institut für Normung, DIN EN 13123-1: Windows, doors and shutters – Explosion resistance – Requirements and classification – Part 1: Shock tube, Beuth, Berlin, 2001.

[9] Century Dynamics Inc., Autodyn: Interactive non-linear dynamic analysis software – Theory Manual 4.0, Horsham, UK, 1998.

[10] Riedel, W., Beton unter dynamischen Lasten, Meso- und makromechanische Modelle und ihre Parameter, Schriftenreihe $\dot{\varepsilon}$ – Forschungsergebnisse aus der Kurzzeitdynamik, Fraunhofer IRB Verlag: Heft 5, 2004.

[11] Johnson, G.R. & Cook, W.H., Fracture characteristics of three metals subjected to various strains, strain rates, temperatures and pressures. *Engineering Fracture Mechanics*, **21**(1), pp. 31–48, 1985.

[12] Klomfass, A., Kranzer, C., Mayrhofer, C. & Stolz, A., A large new shock tube with square test section for the simulation of blast events. *Proceedings of the 22nd MABS – Military Aspects of Blast and Shock*, Bourges, France, 4–9 Nov., 2012.